Angermann et al., http://www.jgp.org/cgi/content/full/jgp.200609507/DC1

DETAILED KINETIC ANALYSIS OF I_{CLCA} RECORDED IN MYOCYTES DIALYZED WITH ATP OR AMP-PNP

Fig. S1 A shows graphs reporting the Ca^{2+} sensitivity of the time constant of activation (τ_{act}) of I_{ClCa} with ATP (filled squares) or AMP-PNP (empty squares) at +70 mV (a), +90 mV (b), +110 mV (c), and +130 mV (d). In the presence of ATP, τ_{act} was Ca^{2+} independent at the voltages examined (slopes were not significantly different from 0 with P values ranging from 0.066 to 0.389). In contrast with AMP-PNP, τ_{act} declined exponentially as a function of pipette [Ca^{2+}], and the values were significantly different from those obtained in ATP for Ca^{2+} concentrations > 250 nM. Fig. S1 B shows graphs reporting the impact of ATP and AMP-PNP on the Ca^{2+} dependence of the time constant(s) of deactivation (τ_{deact}) at −100 mV (a), −50 mV (b), −10 mV (c), and +50 mV (d). Although deactivation was mono-exponential for 250 and 500 nM Ca^{2+} with both nucleotides, deactivation became bi-exponential with 1000 nM Ca^{2+} and ATP, and with 750 nM and 1000 nM Ca^{2+} in the presence of AMP-PNP. For both nucleotides, the slow component of deactivation (τ_{slow}) increased exponentially as a function of pipette [Ca^{2+}] in the negative range of membrane potentials (compare panels Ba, b, and c with panel Bd; the fast component of deactivation τ_{fast} was not plotted for clarity). We also analyzed the voltage dependence of the ratio of the amplitude of the slow over fast ($Amp_{slow/fast}$) components of deactivation with 1000 nM Ca^{2+}. Although this parameter was voltage insensitive between −100 mV and −20 mV for both nucleotides, the analysis revealed a significant increase of this parameter with AMP-PNP vs. ATP (two-way ANOVA yielded $P < 0.001$; unpublished data); e.g., at −100 mV, $Amp_{slow/fast}$ was 0.33 ± 0.06 and 0.60 ± 0.06 ($P < 0.001$) with ATP and AMP-PNP, respectively. Thus, general dephosphorylation slowed deactivation kinetics, especially at higher levels of intracellular Ca^{2+} levels and negative potentials; at 1000 nM Ca^{2+}, in addition to slowing deactivation at negative potentials, dephosphorylation increased the proportion of channels entering slow deactivation in the negative range of membrane potentials.

We also investigated the effects of AMP-PNP on the voltage dependence of I_{ClCa} kinetics and the data are summarized in Fig. S2. Except for ATP and 250 nM Ca^{2+}, where regression analysis revealed a slope significantly different from 0 ($P = 0.035$), τ_{act} did not vary as a function of voltage in cells dialyzed with ATP or AMP-PNP at all pipette [Ca^{2+}] tested ($P \geq 0.298$; Fig. S2 Aa−d). However, τ_{act} was significantly reduced in AMP-PNP–containing myocytes dialyzed with 500 nM Ca^{2+} or higher, and this effect was proportionately greater as pipette [Ca^{2+}] increased. The time constant of deactivation of I_{ClCa} (τ_{deact}) decreased with membrane hyperpolarization in cells dialyzed with ATP and pipette [Ca^{2+}] in the range of 250–750 nM Ca^{2+} (Fig. S2 Ba−c), a result consistent with a previous report from our group in rabbit pulmonary artery myocytes (Greenwood et al., 2001). In contrast, neither the fast (labeled as τ_{fast}) nor the slow decay (labeled as τ_{slow}) of currents evoked by 1000 nM Ca^{2+} exhibited any voltage dependence (Fig. S2 Ba−d). Inhibition of phosphorylation by AMP-PNP increased τ_{deact} significantly regardless of the activator [Ca^{2+}] (Fig. S2 Ba−d). τ_{slow} evoked by 750 and 1000 nM Ca^{2+} was also slower in the presence of AMP-PNP, whereas τ_{fast} was slightly accelerated (Fig. S2 Bd). Although the appearance of τ_{fast} at higher pipette [Ca^{2+}] is unclear, our results indicate that global dephosphorylation in the absence of ATP tends to lock the channel in the open state at negative membrane potentials irrespective of the Ca^{2+} concentration, which is consistent with the observed negative shift in the voltage dependence of I_{ClCa} by AMP-PNP.

JUSTIFICATION FOR THE ADJUSTMENT OF PARAMETERS USED IN OUR COMPUTER SIMULATIONS

Our computer simulations to mimic the behavior of I_{ClCa} in pulmonary arterial myocytes dialyzed with ATP and AMP-PNP were conducted using two mathematical models, each run with their own set of parameters (Table I) to generate the data presented in Figs. 8 and 9. As in our experiments, all simulations were performed in the absence of a Cl^- gradient across the membrane ($E_{Cl} = 0$ mV). Because the affinity of I_{ClCa} for Ca^{2+} was found to be four to five times higher in pulmonary artery myocytes than frog oocytes (Kuruma and Hartzell, 2000), the binding rate constant k_{on} was increased to 20 $M^{-1}s^{-1}$ instead of 3 $M^{-1}s^{-1}$, while a value (50 s^{-1}) identical to that of Kuruma and Hartzell (2000) was used as the unbinding rate constant k_{off}. Although the values used for the rate of channel opening were different, they followed a similar trend to those used by Kuruma and Hartzell (2000), increasing with the number of Ca^{2+} ions bound (Table I). Another distinction from the model used in frog oocytes is that the equations describing the voltage dependence of the rate of channel closure were Boltzmann relationships instead of exponen-

J. Gen. Physiol. © The Rockefeller University Press
http://www.jgp.org/cgi/doi/10.1085/jgp.200609507

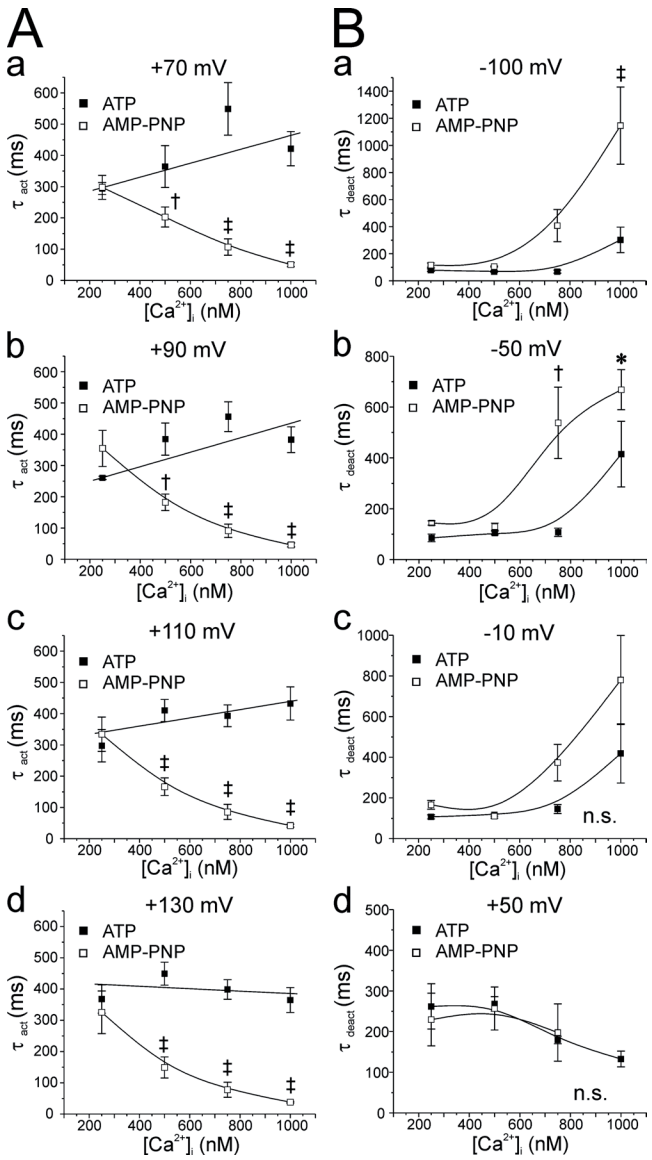

Figure S1. Ca^{2+} dependence of I_{ClCa} kinetics analyzed after 20 min of cell dialysis with ATP and AMP-PNP. (A) Panels a–d show graphs reporting mean ± SEM time constant of activation (τ_{act}) measured after 20 min of cell dialysis with 3 mM ATP (filled squares; $n = 5$–9) or 3 mM AMP-PNP (empty squares; $n = 4$–8) as function of internal Ca^{2+} concentration ($[Ca^{2+}]_i$) at the four distinct step potentials indicated: +70 mV (a), +90 mV (b), +110 mV (c), and +130 mV (d). Time constants were determined by exponential curve fitting of the time-dependent component of I_{ClCa} elicited during 1-s depolarizing steps from HP = −50 mV (see Fig. 3). The straight lines passing through all datasets obtained in ATP are linear regression fits whose slopes were all not significantly different from 0 ($P > 0.05$), indicating lack of Ca^{2+} dependence. All lines passing through the AMP-PNP datasets are B-Spline fits estimated by Origin software. Two-way ANOVA tests revealed significant differences at all potentials examined between ATP and AMP-PNP ($P < 0.01$); post-hoc tests: †, $P < 0.01$; ‡, $P < 0.001$. (B) Panels a–d show plots reporting mean ± SEM time constant of deactivation (τ_{deact}) measured after 20 min of cell dialysis with 3 mM ATP (filled squares; n = 3-7) or 3 mM AMP-PNP (empty squares; $n = 2$–9) as function of internal pipette Ca^{2+} concentration ($[Ca^{2+}]_i$) at the four representative step potentials indicated: −100 mV (a), −50 mV (b), −10 mV (c), and +50 mV (d). Time constants were determined by exponential curve fitting of I_{ClCa} tail currents. The double-pulse protocol used to elicit tail currents consisted of a constant 1-s step to +100 mV followed by a 1-s return step ranging from −100 to +50 mV applied in 10-mV increments from HP = −50 mV. As explained in the text, deactivation was bi-exponential with ATP and 1000 nM Ca^{2+}, and with AMP-PNP and 750 nM and 1000 nM Ca^{2+}. Only the slow time constant of deactivation is reported in this graph for the sake of clarity. The lines passing through all datasets are B-Spline fits estimated by Origin software. Two-way ANOVA tests revealed significant differences at all potentials examined between ATP and AMP-PNP ($P < 0.01$) except +50 mV (n.s., not significant); post-hoc tests: *, $P < 0.05$; †, $P < 0.01$; ‡, $P < 0.001$. All plots were generated from data obtained after 20 min of cell dialysis with either nucleotide.

tial functions. This was necessary to describe the sigmoidal nature of the voltage dependence of the Ca^{2+} affinity curves determined in our experiments (Fig. 5 A). The voltage dependence of the function determining β_x was progressively made more negative with Ca^{2+} binding (Table I) to account for the negative shift in the voltage dependence of I_{ClCa} conductance (Fig. 6 A). The steepness of the Boltzmann relationships describing β_x was set to a constant value of 50 mV (Table I) for both models and is similar to the range of values estimated from experiments (Fig. 6 A, inset). The gating variable of the O_2 and O_3 states for the ATP model was set to 0 instead of 1 in the AMP-PNP model. As described in the next supplementary section, this procedure greatly attenuated the steep Ca^{2+} dependence of the time constant of activation of I_{ClCa} observed with AMP-PNP, which was Ca^{2+} independent in cells dialyzed with ATP (Fig. S1). Setting these states to 0 allowed for locking a fraction of the channels in the "closed" or "blocked" state at $[Ca^{2+}]_i$, thus opposing the activating effect of Ca^{2+} on I_{ClCa} kinetics, as described in the following section.

COMPARISON OF KINETICS OF I_{CLCA} ANALYZED FROM EXPERIMENTAL AND MODELED DATA

As mentioned in the text, our models reproduced well the Ca^{2+} and voltage dependence of I_{ClCa} and how these properties are modulated by global phosphorylation status. We also performed a superficial comparison of kinetic data derived from actual experiments and our computer models. For example with 500 nM Ca^{2+}, τ_{act} at +120 mV was 216 ms (actual data: 432 ± 28 ms, $n = 7$) and 193 ms (actual data: 163 ± 27 ms, $n = 7$), respectively, with ATP and AMP-PNP; τ_{deact} at −50 mV was 54 ms (actual data: 105 ± 7 ms, $n = 6$) with ATP and 139 ms for the slow component

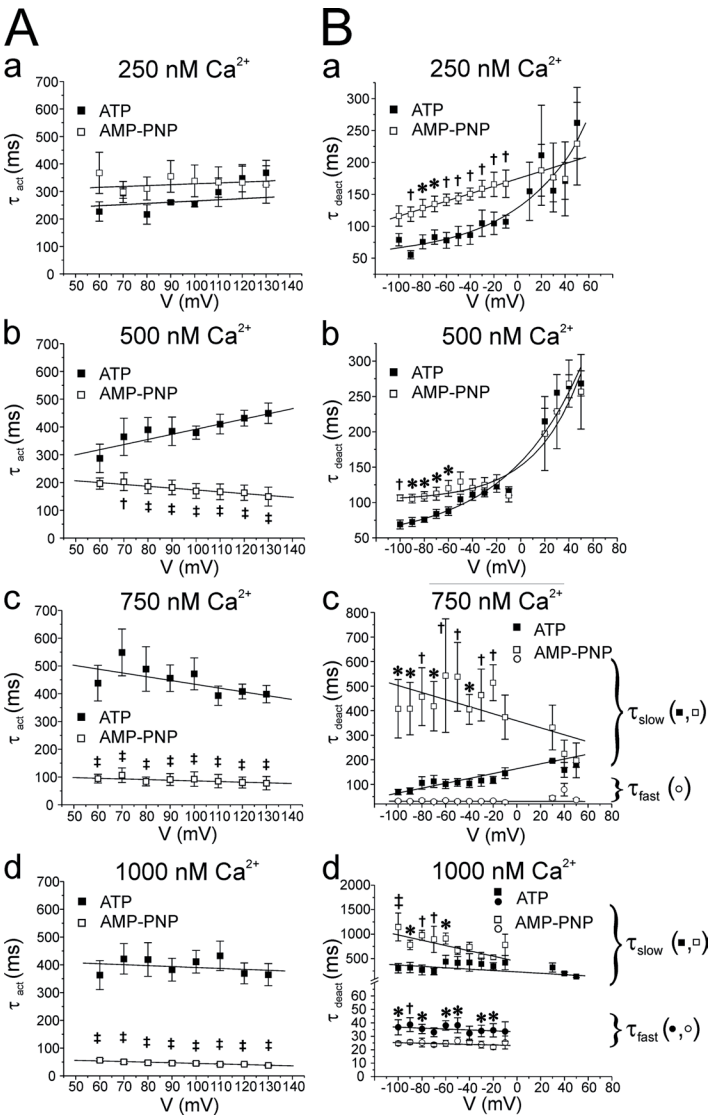

Figure S2. Voltage dependence of I_{ClCa} kinetics analyzed after 20 min of cell dialysis with ATP and AMP-PNP. (A) Panels a–d show graphs reporting mean ± SEM time constant of activation (τ_{act}) measured after 20 min of cell dialysis with 3 mM ATP (filled squares; n = 4–8) or 3 mM AMP-PNP (empty squares; n = 4–8) as function of step potential at the four Ca^{2+} concentrations indicated: 250 nM (a), 500 nM (b), 750 nM (c), and 1000 nM (d). Time constants were determined by exponential curve fitting of the time-dependent component of I_{ClCa} elicited during 1-s depolarizing steps from HP = −50 mV (see Fig. 3). All straight lines through the data points are linear regressions. Except for 250 nM Ca^{2+}, two-way ANOVA analyses revealed significant differences between ATP and AMP-PNP datasets ($P < 0.001$); post-hoc tests: †, $P < 0.01$; ‡, $P < 0.001$. (B) Panels a–d show plots reporting mean ± SEM time constant(s) of deactivation (τ_{deact}) measured after 20 min of cell dialysis with 3 mM ATP (filled symbols; n = 2-8) or 3 mM AMP-PNP (empty symbols; n = 2-9) as function of step potential at the four Ca^{2+} concentrations indicated: 250 nM (a), 500 nM (b), 750 nM (c), and 1000 nM (d). Time constants were determined by exponential curve fitting of I_{ClCa} tail currents. The double-pulse protocol used to elicit tail currents consisted of a constant 1-s step to +100 mV followed by a 1-s return step ranging from −100 to +50 mV applied in 10-mV increments from HP = −50 mV. As explained in the text, deactivation was bi-exponential with ATP and 1000 nM Ca^{2+} (n = 5–7), and with AMP-PNP and 750 nM (n = 2–5) and 1000 nM Ca^{2+} (n = 2–9). Fast (τ_{fast}) and slow (τ_{slow}) time constants of deactivation are labeled as circles and squares, respectively. Except for the data with ATP and 250 nM and 500 nM Ca^{2+}, and with AMP-PNP and 500 nM Ca^{2+}, which are exponential fits to the data, all other lines are linear regressions. For all groups of data, two-way ANOVA analyses revealed significant differences between ATP and AMP-PNP with $P < 0.05$; post-hoc tests: †, $P < 0.01$; ‡, $P < 0.001$. Some, but not all, mean data points presented here are reproduced from Fig. 8 but plotted differently. All plots were generated from data obtained after 20 min of cell dialysis with either nucleotide.

with AMP-PNP (actual data: 130 ± 14 ms, n=8). As for our data, the time constants of activation measured with ATP (421 ms) and AMP-PNP (431 ms) were similar with 250 nM Ca^{2+}; with 500 nM Ca^{2+}, τ_{act} declined to ?220 ms with ATP and to ?190 ms with AMP-PNP, but stabilized at higher [Ca^{2+}] with ATP (τ_{act} = 181 ms and 182 ms with 750 nM and 1000 nM Ca^{2+}, respectively), whereas it continued to decline exponentially with AMP-PNP (τ_{act} = 124 ms and 88 ms with 750 nM and 1000 nM Ca^{2+}, respectively; see Fig. S1 A). Moreover, deactivation at −50 mV with ATP was only bi-exponential at 1000 nM Ca^{2+}, whereas the sum of two exponentials was required to adequately fit deactivation with AMP-PNP at [Ca^{2+}] ≥ 500 nM. The range of values for τ_{fast} and τ_{slow} were also semi-quantitatively similar to real data; e.g., simulated data with 750 nM Ca^{2+} and AMP-PNP yielded values for τ_{fast} and τ_{slow} of 32 and 137 ms, compared with 31 ± 4 ms (n = 5) and 538 ± 140 ms (n = 5) for experimental data. Finally, although not analyzed in details, both the ATP and AMP-PNP models also reproduced, at least semi-quantitatively, the Ca^{2+} (Fig. S1 B) and voltage dependence (Fig. S2) of deactivation of I_{ClCa}.

REFERENCES

Greenwood, I., J. Ledoux, and N. Leblanc. 2001. Differential regulation of Ca^{2+}-activated Cl^- currents in rabbit arterial and portal vein smooth muscle cells by Ca^{2+}-calmodulin–dependent kinase. *J. Physiol.* 534:395–408.

Kuruma, A., and H.C. Hartzell. 2000. Bimodal control of a Ca^{2+}-activated Cl^- channel by different Ca^{2+} signals. *J. Gen. Physiol.* 115:59–80.